Biophysical Journal

Article



On the stability and layered organization of protein-**DNA** condensates

Andrew P. Latham¹ and Bin Zhang^{1,*}

¹Department of Chemistry, Massachusetts Institute of Technology, Cambridge, Massachusetts

ABSTRACT Multi-component phase separation is emerging as a key mechanism for the formation of biological condensates that play essential roles in signal sensing and transcriptional regulation. The molecular factors that dictate these condensates' stability and spatial organization are not fully understood, and it remains challenging to predict their microstructures. Using a near-atomistic, chemically accurate force field, we studied the phase behavior of chromatin regulators that are crucial for heterochromatin organization and their interactions with DNA. Our computed phase diagrams recapitulated previous experimental findings on different proteins. They revealed a strong dependence of condensate stability on the protein-DNA mixing ratio as a result of balancing protein-protein interactions and charge neutralization. Notably, a layered organization was observed in condensates formed by mixing HP1, histone H1, and DNA. This layered organization may be of biological relevance, as it enables cooperative DNA packaging between the two chromatin regulators: histone H1 softens the DNA to facilitate the compaction induced by HP1 droplets. Our study supports near-atomistic models as a valuable tool for characterizing the structure and stability of biological condensates.

SIGNIFICANCE Eukaryotic cells are compartmentalized into membraneless organelles for efficient signal sensing and transcriptional regulation. Multi-component phase separation has been proposed as the mechanism for organelle formation. We carried out an extensive set of simulations to study the phase behavior of chromatin regulators that are essential for heterochromatin organization and their interactions with DNA. Our study provides critical insight into the molecular factors that dictate protein-DNA condensates' stability. We further reveal novel microstructures of these condensates that have profound implications on chromatin packaging in vivo.

INTRODUCTION

Compartmentalization allows eukaryotic cells to coordinate biochemical reactions with high specificity and efficiency. In addition to traditional membrane-enclosed compartments, recent studies have uncovered a variety of membraneless organelles (1-4). These organelles are dynamic and can adjust their composition in response to ligand binding and chemical modifications (5), rendering them ideal designs for signal sensing (6). Membraneless organelles are prevalent in the cytosol, with examples including P granules (7) and stress granules (8). They are frequently found in the nucleus as well (9) and may underlie the organization of heterochromatin (10–12), superenhancers (13), nuclear speckles (14,15), and nucleoli (16,17). These organelles are often enriched

Submitted October 20, 2021, and accepted for publication March 24, 2022.

*Correspondence: binz@mit.edu

Editor: Tamar Schlick.

https://doi.org/10.1016/j.bpj.2022.03.028

© 2022 Biophysical Society.

with intrinsically disordered proteins (IDPs) (18,19), which may drive condensate formation via liquid-liquid phase separation (LLPS) (20,21).

Besides IDPs, membraneless organelles often contain RNA and DNA molecules (20–22). The complex phase behavior of such multi-component systems is becoming increasingly appreciated (23,24). The presence of nucleotides may induce the phase separation of IDPs that do not form condensates on their own via polymer-polymer phase separation (25–28) or bridge-induced phase separation (29-31). These additional mechanisms can give rise to phenomena not present in protein-only systems, including the so-called re-entrant phase separation (32,33). Multiple component phase separation also supports novel outcomes. For example, the condensate composition and the molar fraction of individual components can be fine-tuned by adjusting their interaction strength (24,34). Rather than a homogeneous mixture, droplets may instead exhibit a layered organization with subcompartments, which has indeed been observed in nucleoli (16) and speckles (35). Please cite this article in press as: Latham and Zhang, On the stability and layered organization of protein-DNA condensates, Biophysical Journal (2022), https:// doi.org/10.1016/j.bpj.2022.03.028

Latham and Zhang

Finally, multiple demixed droplets without interfacial contacts can also form (36-38).

General principles of multi-component phase separation are beginning to emerge (23,24). Electrostatic interactions between charged molecules have received great attention, and the complex coacervation mechanism serves as a powerful theoretical framework for studying condensate stability (27,28). Jacobs and Frenkel showed that demixed states could form in the presence of large fluctuations of intermolecular interaction strengths, facilitating the coexistence of multiple organelles (36). In addition to demixed states, Pappu and coworkers further found that single condensates, but with layered organization and subcompartments, could form for certain interaction patterns (16,39,40). The precise morphology of the droplet with multiple coexisting phases is dependent on their interfacial tension and volume fractions (41). Despite these advances in understanding multi-component phase separation, predicting the microstructures of the multi-component condensates remains challenging. The variety of possible outcomes in spatial organization places a high demand on the model accuracy.

In this work, we simulated LLPS and the organization of multi-component systems with a near-atomistic model. We focused on the phase behavior of chromatin regulators that play crucial roles in heterochromatin formation and gene silencing, including heterochromatin protein 1 (HP1) and histone H1 (2,42). A recently developed force field, MOFF (43,44), which is well suited for simulating both ordered and disordered proteins, was combined with a chemically accurate DNA model (45) to study protein-DNA condensates. Our simulations resolved the difference of various chromatin regulators in their phase behaviors and their association with DNA molecules. A linear model that accounts for both protein-protein interactions and system net charges can quantitatively reproduce the critical temperature for various systems and provides insight into the stability of biological condensates. Furthermore, DNA molecules can act as bridging agents to support layered organization in ternary systems that mix them with $HP1\alpha$ and H1. Such a layered organization promotes collaboration between the two chromatin regulators to compact DNA and possibly package heterochromatin. Our study on HP1 homologs further supports a model proposed by Keenen et al. (46) in which the formation of heterodimers may destabilize $HP1\alpha/DNA$ condensates. We conclude that near-atomistic modeling is useful for predicting the microstructures and phase behavior of multi-component systems and uncovering the design principles of biomolecular condensates.

MATERIALS AND METHODS

Near-atomistic protein-DNA force fields

Simulating large-scale phenomena such as LLPS necessitates balancing computational expense with model resolution. We represented protein and DNA molecules with one coarse-grained bead per amino acid or nucleotide. Models of similar resolutions have been widely used to study IDPs (47-53) and protein-DNA complexes (54-62) with great success. The MOFF force field for proteins (43) and molecular renormalization group coarse-graining model (MRG-CG) for the DNA (45) were combined together to describe protein-DNA interactions under implicit solvation. Each model is described briefly below, with full details provided in the supporting material. An implementation of our force field can be found at the group GitHub page.

The potential energy for a protein structure r in MOFF is defined as

$$U_{\text{MOFF}}(\mathbf{r}) = U_{\text{backbone}} + U_{\text{memory}} + U_{\text{electrostatics}} + U_{\text{contact}}.$$
 (1)

The first two terms are responsible for maintaining the backbone geometry and secondary structures of protein molecules. Equilibrium distances and angles used in defining these potentials were determined from initial structures built with RaptorX (63). $U_{\text{electrostatics}}$ describes electrostatic interactions between charged residues with the Debye-Hückle theory and a distance-dependent dielectric constant. The last term U_{contact} is the amino acid type-dependent pairwise contact potential optimized to reproduce the radius of gyration for a list of folded and disordered proteins and sculpt a funneled energy landscape for folded proteins. The contact potential captures non-bonded potentials beyond charge-charge interactions, including hydrogen bonds, π - π stacking, hydrophobic interactions, and cation- π interactions. In addition, for proteins with folded domains, structure-based potentials (64) were introduced to stabilize tertiary contacts. The strength of these potentials was tuned to reproduce the root-mean-squared fluctuations estimated with all-atom simulations (Fig. S1).

The potential energy of the MRG-CG DNA model takes the form

$$U_{\rm DNA}(\mathbf{r}) = U_{\rm bond} + U_{\rm fan} + U_{\rm angle} + U_{\rm electrostatics} + U_{\rm EV}.$$
 (2)

 $U_{\rm bond}, U_{\rm fan}$, and $U_{\rm angle}$ account for local interactions among nearby nucleotides, while $U_{\text{electrostatics}}$ and U_{EV} correspond to non-bonded, electrostatic interactions and the excluded volume effect. While the original model was parameterized with explicit ions, we switched to implicit ions to be consistent with the electrostatic potential defined in the protein force field. After adjusting the strength of local interactions, we found that the implicit ion model succeeded in predicting the DNA persistence length at the physiological salt concentration (Fig. S2).

Protein-DNA interactions included electrostatic and excluded volume contributions. Electrostatic interactions between charged residues and nucleotides were again modeled with the Debye-Hückle theory and a distance-dependent dielectric constant as the $U_{
m electrostatics}$ term in MOFF. The excluded volume potential ensures amino acids remain at least 0.57 nm away from nucleotides. This treatment worked well at reproducing the experimental binding free energies for various protein-DNA complexes (Fig. S3). We note that the DNA model employed here does not account for sequence effects and will miss specific protein-DNA interactions besides electrostatics. Further improving the force field accuracy in the future may allow more quantitative evaluations of condensate stability.

Molecular dynamics simulation details

We used the slab simulation technique to probe the thermodynamic stability of condensates and determine the critical temperature (T_C) (43,48,65). Constant temperature molecular dynamics simulations were performed using the software GROMACS (66) with a time step of 10 fs. Simulations were initialized with a high-density protein phase in the center of the simulation box. After expansion along the z dimension of the simulation box, the highdensity protein phase becomes a dense slab that is periodic in x and y, but does not interact with its periodic image in z due to the size of the box. The lack of periodic interactions in the z direction allows the formation of two

interfaces between a dense biopolymer phase and a dilute vapor (implicit solvent) phase. Each simulation lasted for 2 µs, and Langevin dynamics was used to control the temperature. Protein concentrations of the two phases collected from simulations at different temperatures were used to construct the temperature-concentration phase diagram and determine the critical temperature. Additional simulation details can be found in supporting material under "computing phase diagrams with slab simulations."

We evaluated the robustness of the estimated critical temperature with respect to system size, simulation length, and initial configurations (Fig. S4). The standard deviation calculated across different simulations is 5.1 K, far smaller than the difference in $T_{\rm C}$ across systems. Therefore, the simulation protocol suffices for quantitatively evaluating the condensate stability.

We fixed the total number of molecules, including HP1 dimers, H1 monomers, and double-stranded DNA (dsDNA), to be 100 for all slab simulations at different protein-DNA mixing ratios. The dsDNA used in these simulations is 50 bp long, a length that is short enough to avoid interactions with its periodic image but long enough to bind H1 and HP1. The exact protein-DNA ratios and temperatures of our simulations are provided in Table S1.

In addition to slab simulations, we studied the effect of protein phase separation on DNA conformation. These simulations began with a strand of 200-bp-long dsDNA bound to a droplet of 100 HP1 α dimers inside a cubic box. We further introduced H1 or HP1 β at various concentrations before carrying out 10-µs-long constant temperature simulations at 300 K. The first 1 µs of these simulations was discarded for equilibration, leaving 9 μ s of data to analyze. While the droplet stability in these types of simulations is more susceptible to finite size effects than the slab simulations (65), they are still helpful for probing the collective impact of chromatin regulators on DNA conformation. These simulations are described in full in the supporting material under "probing the impact of phase separation on DNA conformation."

RESULTS

Near-atomistic modeling resolves the distinct phase behavior of chromatin regulators

To study multi-component LLPS of biological significance, we characterized the phase behavior of three chromatin regulator proteins, HP1 α , HP1 β , and histone H1 (Fig. 1; Tables S1 and S2), with DNA. All proteins consist of both folded and disordered regions. The two folded domains of HP1 include a chromodomain (CD) that recognizes methylated N-terminal tails of histone H3 (H3K9me3) and a chromoshadow domain (CSD) that enables dimerization (67–69). The globular domain of H1 was frequently found to bind near nucleosome dyad and contact linker DNA (42,70). Meanwhile, the disordered regions in these proteins can drive their LLPS when mixed with DNA (25,46,71,72). As such, they serve as ideal model systems to investigate how interactions between proteins and nucleic acids contribute to the stability of biological condensates.

Structural characterization of chromatin regulators is challenging, and their inclusion of both folded and disordered domains places a high demand on the force field accuracy. We previously introduced MOFF (43,44), a coarse-grained protein force field that succeeds in predicting the size of disordered proteins and in folding certain globular proteins. When applied to HP1 α and HP1 β , MOFF predicted the radius of gyration (R_g) with values that match small-angle X-ray scattering results.

Furthermore, the computational efficiency of such a coarse-grained model allows for the investigation of protein phase behavior by computing phase diagrams via slab simulations (see methods and Fig. S5 in the supporting material). These diagrams trace the polymer concentration of coexisting condensed and dilute phases at different temperatures. The critical temperature provides a quantitative evaluation of the phase separation tendency, and a value above 300 K suggests that the system will form stable condensates at room temperature.

Consistent with the observation that $HP1\alpha$ can phase separate more readily than HP1 β (10,12,73,74), the $T_{\rm C}$ for

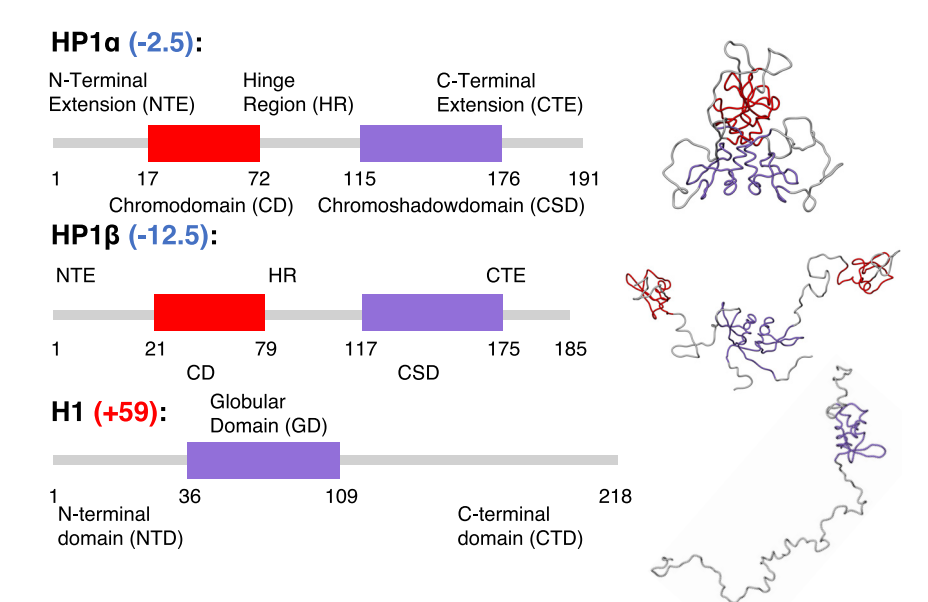


FIGURE 1 Sequence and structural features of the three chromatin regulators. The boxes indicate folded domains while gray lines correspond to disordered regions. Numbers in parentheses represent the net charge of each protein. The structures shown on the right are the most likely conformations determined from simulations (43) and include dimers for HP1 proteins and a monomer for H1. To see this figure in color, go online.

Please cite this article in press as: Latham and Zhang, On the stability and layered organization of protein-DNA condensates, Biophysical Journal (2022), https://doi.org/10.1016/j.bpj.2022.03.028

Latham and Zhang

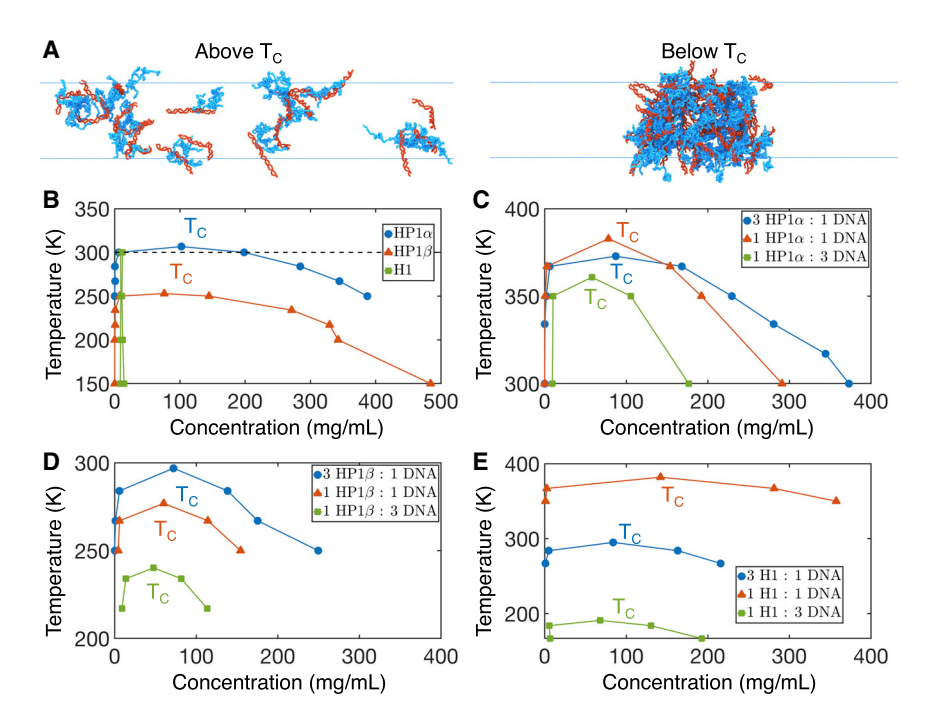


FIGURE 2 Phase diagrams of proteins and protein-DNA mixtures. (A) Example configurations of 1 HP1 α (blue):1 DNA (red) above and below $T_{\rm C}$. (B) Phase diagrams of protein systems without DNA. The small concentration values for H1 indicate that it does not phase separate on its own. Results for HP1 homologs are adapted with permission from (43). Copyright 2021, American Chemical Society. (C–E) Phase diagrams and critical temperatures of HP1 α (C), HP1 β (D), and H1 (E) at different mixing ratios with DNA. To see this figure in color, go online.

HP1 α determined using MOFF is higher than that for HP1 β (Fig. 2 B). On the other hand, we found that histone H1 does not phase separate under all conditions we tested. This result is in agreement with previous experiments (71,75) and is likely due to H1's large net positive charge.

We further combined MOFF with the MRG-CG DNA model (45) to study the impact of DNA molecules on protein phase separation. Accounting for the DNA is crucial for a more biologically relevant scenario, since chromatin regulators primarily reside inside the nucleus filled with DNA. Numerous studies have shown that DNA could significantly alter both the thermodynamics and kinetics of phase separation (76–78). The DNA model represents each nucleotide with one bead and reproduces the persistence length at the physiological salt concentration (Fig. S2). Protein-DNA interactions were adjusted to reproduce the binding free energy for a set of complexes (Fig. S3). With this calibrated force field and the slab simulation methodology (43,65), we constructed phase diagrams for each protein at different ratios of protein (dimers of HP1 or monomers of H1) to a 50-bp-long DNA while keeping the total number of molecules fixed at 100.

The three proteins exhibit striking differences in their interaction with DNA molecules (Fig. 2). In agreement with experimental findings, HP1 α and H1, but not HP1 β , can phase separate at room temperature at certain protein-DNA ratios (10,25,46). Notably, the response of $T_{\rm C}$ to DNA concentration varies dramatically from protein to protein. HP1 α favors an equal protein to DNA ratio (1HP1 α :1DNA), but these effects are relatively subtle, and the $T_{\rm C}$ stays between 361 K and 383 K for all mixing ratios. On the other hand, while H1 similarly favors the equal mix-

ing ratio, its critical temperature changed from 382 K at 1H1:1DNA to 191 K at 1H1:3DNA. Indeed, experiments have shown that similar ratios are favored for both HP1 α and H1 (25,46). Meanwhile, 3HP1 β :1DNA is preferred over other setups.

Sequence-specific interactions and charge balance dictate condensate stability

The apparent disparity in the protein-DNA ratio of the most stable condensates motivated us to search for a better theoretical understanding of their stability. One possible quantity of importance is the net system charge, Q. Through a complex coacervation mechanism (27,79) for which electrostatic interactions between oppositely charged polyelectrolytes dominate the system, low levels of DNA can enhance condensate formation, whereas high levels can cause their dissolution. The optimal DNA ratio for maximum stability is expected to neutralize the overall charge of the condensate (32–34). While it may explain the results for H1, the charge-balance mechanism fails to reconcile the differences across proteins. In particular, HP1 molecules are negatively charged themselves and cannot approach a neutral droplet (Fig. 3 A), but nevertheless form more stable condensates with DNA than H1. As such, more refined mechanisms must be utilized to understand the properties of these condensates.

One key component ignored in the above charge-balance argument is the short-range van der Waals interactions between protein molecules. From the Flory-Huggins theory of mixing for polymer solutions (80), it is well known that

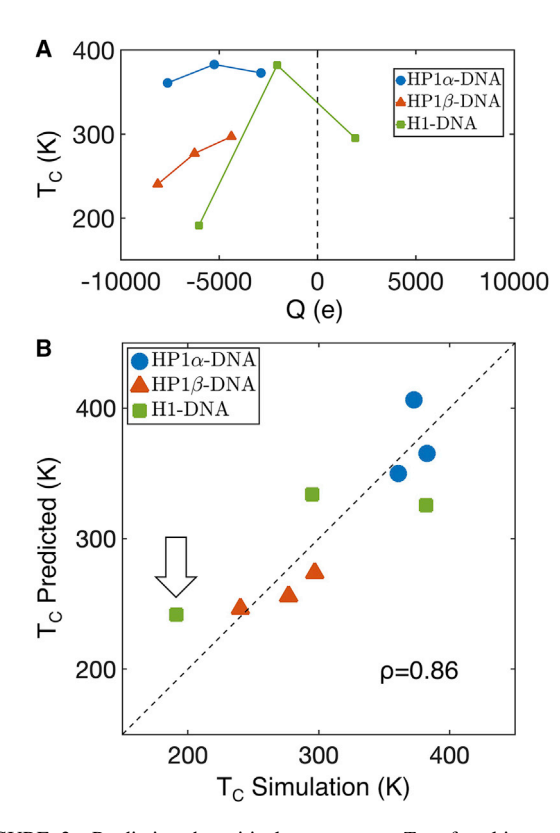


FIGURE 3 Predicting the critical temperature, $T_{\rm C}$, of multi-component phase separation. (A) $T_{\rm C}$ as a function of the net system charge (Q) for the three chromatin regulators mixed at different ratios with DNA molecules. (B) Comparison between simulated $T_{\rm C}$ and values obtained through linear regression, given in Eq. 3. ρ is the Pearson correlation coefficient between the two data sets, and the dashed diagonal line is provided as a guide to the eye. The arrow draws attention to the largest outlier, 1H1:3DNA. To see this figure in color, go online.

 $T_{\rm C}$ depends linearly on the interaction energy between proteins, E_{pp} . Therefore, we included both factors in a linear regression model to fit $T_{\rm C}$ estimated from slab simulations

$$T_{\rm C}/K = 13.27 \times E_{\rm pp} + 2.60 \times 10^5 \times |Q|^{-1} + 234.$$
 (3)

We estimated E_{pp} from the binding free energy curves for two HP1 dimers or two H1 monomers (Fig. S6).

This linear model for $T_{\rm C}$ fits our data well (Fig. 3 B), while neither Q nor E_{pp} alone can provide fits of comparable quality (Fig. S7). Furthermore, it provides an intuitive explanation of our simulated trends. For example, HP1 α -DNA condensates are stable across many protein-DNA ratios due to the strong protein-protein interactions and $HP1\alpha$'s relatively small net charge. In comparison, condensates formed with HP1 β are less stable as the corresponding $E_{\rm pp}$ is negative, and the protein is more negatively charged. Finally, the strong dependence of H1-DNA condensate stability on the protein-DNA ratio arises from the competition between the repulsive H1-H1 and attractive protein-DNA interactions.

However, given its simplicity, we do not expect the linear model to account for all the complex behaviors of protein-DNA condensates. In particular, a mean-field model of the electrostatic contribution to the free energy based on charge density is insufficient for polyelectrolytes (81). The polymer connectivity places significant constraints on charge distribution. Both HP1 α and HP1 β bind favorably with DNA despite their overall negative charge (Fig. S8). Therefore, the simple dependence on net charge cannot explain the enhanced phase separation upon introducing DNA because of favorable protein-DNA interactions. In addition, the tight binding between histone H1 and DNA may give rise to magic number effects (82,83), which can become more apparent as the length of DNA molecules is varied. Contributions from configurational entropy to phase separation in such systems become essential but are not captured by either $E_{\rm pp}$ or Q. Therefore, H1 systems often appear as outliers of the linear fit.

DNA bridging drives layered organization in ternary systems

As they coexist inside the nucleus, chromatin regulators may cooperate or compete when binding with DNA. Prior in vivo studies have suggested that HP1 and H1 localize together in heterochromatic regions (75). The microscopic structures of such ternary systems are poorly characterized. Recent studies have shown that three-component systems with solvent can give rise to complex multi-phase scenarios, including demixed droplets, a condensed homogenous phase, or a layered organization with subcompartments (39,84). We determined the temperature-density phase diagrams for ternary complexes to study both their structural organization and stability.

We performed slab simulations with 1HP1 α :1H1:2DNA and $1HP1\alpha:1HP1\beta:2DNA$ at various temperatures to probe the density of condensed and dilute phases (see Table S1 for simulation details). As shown in Fig. 4, both systems display upper critical temperatures comparable with 1HP1 α :1DNA. Therefore, H1 and HP1 β do not seem to impact the stability of condensates formed by HP1 α and DNA. This observation is in strong contrast to the phase diagrams of protein-only mixtures. As shown in Fig. S9, both H1 and HP1 β destabilize condensates formed only with HP1 α , preventing LLPS at room temperature. The destabilizing effect likely stems from the repulsive interactions between H1-H1 and HP1 β - $HP1\beta$ (Fig. S6). The shape of the ternary complex phase diagrams also appears different from that of protein-DNA condensates shown in Fig. 2. For example, two regimes can often be seen. The two regimes are particularly visible for $1HP1\alpha:1HP1\beta:2DNA$, supporting the definition of two critical temperatures (Fig. S10).

We further examined the structures to better understand the stability of the ternary mixtures and interpret the phase diagrams. At low temperatures, both systems formed a Latham and Zhang

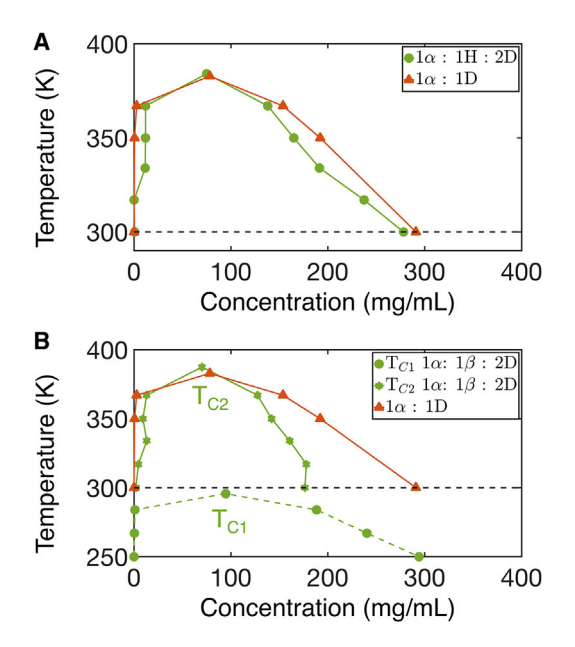


FIGURE 4 Phase diagrams of ternary systems with implicit solvation for HP1α-H1-DNA (A) and HP1α-HP1β-DNA (B) mixtures. Abbreviations are used for different biomolecules (α , HP1 α ; H, H1; D, DNA; β , HP1 β). The result for 1HP1α:1DNA is included for comparison. To see this figure in color, go online.

layered organization, which corresponds to a demixed state with two contacting liquid phases that differ in their relative composition (39). The layered organization can be readily seen in the z-density profile of the simulated condensates. For both systems, HP1 α is concentrated in the middle of the slab, with H1 or HP1 β residing at the exterior (Fig. 5, A and C). The inclusion of DNA in both liquids reduces the interfacial tension between them to prevent complete separation. The stability of the two systems differs dramatically, however. For example, the condensate with H1 remains stable at 300 K, supporting the biological relevance of the layered organization. On the other hand, the condensate with HP1 β tends to shed off HP1 β at high temperatures, resulting in more homogeneous phases that are increasingly enriched with HP1 α (Fig. 5 D). We note that, because of our use of a finite number of molecules and the challenges associated with sampling these systems with strong electrostatic interactions, the estimated density profiles exhibit asymmetry along the z axis. Nevertheless, we found that doubling the system size and improving simulation convergence preserved the layered organizations shown in Fig. 5, supporting their significance (Fig. S11).

Overall, the condensates of these ternary systems are made up of two liquid phases enriched and depleted of $HP1\alpha$. Their temperature-density phase diagrams can indeed be understood from studies on partially miscible liquids (85). For HP1 α -HP1 β -2DNA, the system first undergoes a "boiling" process to dissociate HP1β/DNA complexes at T_{C1} (see Figs. 4 B and 5 D). The second transition corresponds to the vapor-liquid phase separation of HP1 α and DNA, and the corresponding T_{C2} is comparable with that of the binary mixtures. On the other hand, the two phases in HP1-H1-2DNA become more miscible at higher temperatures before the whole condensate falls apart, and the boiling transition is less evident. The difference between the two systems partially arises from the more favorable interaction between HP1 α and H1 than that between $HP1\alpha$ and $HP1\beta$ (Fig. S12).

Layered organization facilitates DNA softening and compaction

While slab simulations combined with phase diagrams can highlight the diverse interactions that drive phase separation, they provide little information regarding the impact of liquid droplets on chromatin conformation due to our use of short DNA segments. Cellular environments likely mirror a single long DNA strand, the conformation of which may depend strongly on the contacting chromatin regulators (45). To examine whether the condensates studied here can compact chromatin to restrict DNA accessibility, we performed simulations for a 200-bp-long DNA in the presence of protein droplets. While chromatin differs from naked DNA due to its incorporation of histone proteins, the simulations may nevertheless provide insight into the impact of polymer connectivity on phase separation and vice versa.

Starting from a conformation with 100 HP1 dimers positioned next to the DNA molecule, we performed long-timescale simulations to equilibrate the system. We found that $HP1\alpha$ condensed onto the DNA (Figs. 6 A and S13 A), resulting in a large droplet that incorporates most proteins and remains stable throughout the simulation time (Figs. 6 C and S14). The protein droplet induced highly bent DNA configurations (Fig. 6 A), giving rise to a second maximum at smaller values in the distribution of the DNA end-to-end distance (Fig. S13 B). Notably, similarly collapsed DNA configurations do not appear metastable upon binding of one or two HP1 α dimers (Fig. S15), indicating the importance of a collective role by many proteins in bending the DNA. DNA bending by $HP1\alpha$ droplets has indeed been observed by Keenen et al. using single-molecule DNA curtain experiments (46). However, a quantitative comparison between simulation and experimental results may be challenging, since the absolute stability of the collapsed DNA configuration depends on both the DNA length and the protein concentration.

To examine how HP1α-H1 mixtures might affect DNA conformations, we performed simulations with varying additional amounts of H1: from 100 to 6 monomers. Consistent with those presented in Fig. 5, the single-DNA simulations also resulted in layered organizations, with HP1 condensates surrounding DNA-bound H1 (Fig. 6 B). However, due to their stronger binding affinity (Fig. S8), H1 molecules essentially cover the entire DNA. At high concentrations, H1 can even strip HP1 α away from the

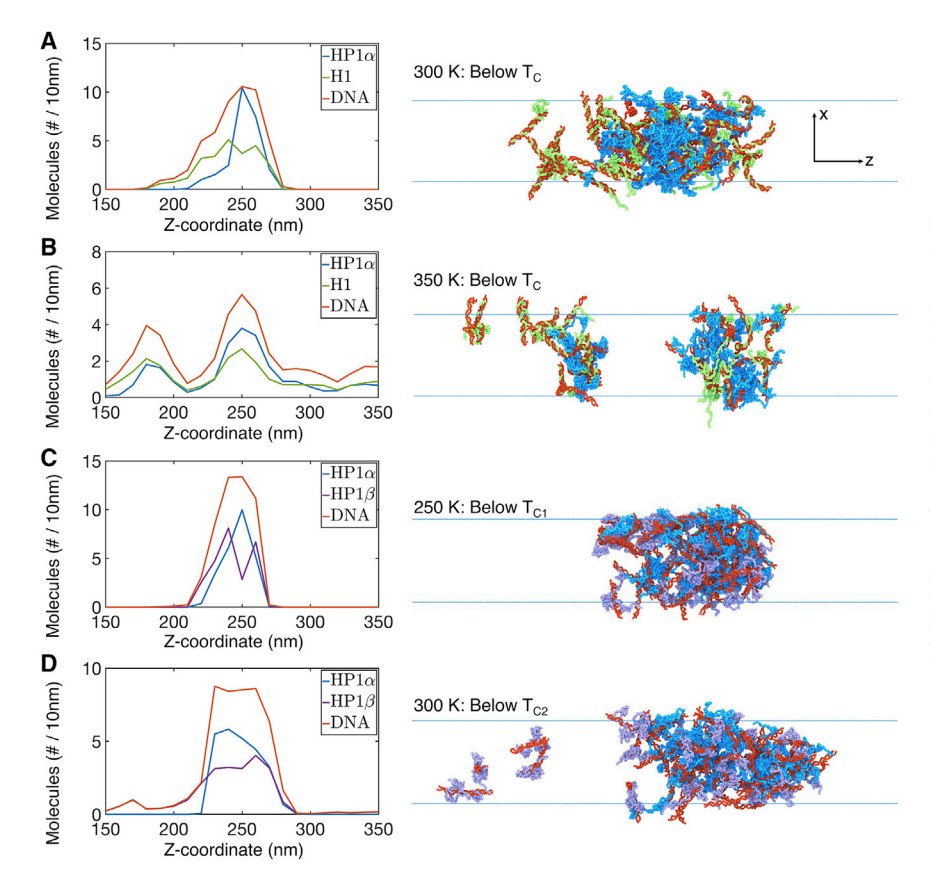


FIGURE 5 Slab density profiles support layered organizations in ternary mixtures. (A) At 300 K for 1HP1 α (blue):1H1 (green):2DNA (red), HP1 α coalesces toward the center of the droplet, with H1 to the outside. (B) Still below T_C for 1HP1α:1H1:2DNA at 350 K, the layered organization becomes less evident and molecules are more uniformly distributed in the condensate. The condensate also becomes less stable and undergoes multiple fusion and merging events during the simulation. An example configuration with two broken clusters is shown on the right. (C) Below $T_{\rm C1}$ (250 K) for 1HP1 α (blue):1HP1 β (purple):2DNA (red), HP1 α coalesces toward the center of the droplet, with HP1 β to the outside. (D) Below T_{C2} (300 K) for 1HP1 α :1HP1 β :2DNA, $HP1\beta/DNA$ complexes begin to fall off the condensate, leaving behind a state enriched in HP1 α . To see this figure in color, go online.

DNA (Fig. S13 A), reducing HP1 α 's participation in droplet formation (Fig. 6 C).

In addition to forming layered organizations, we noticed that introducing H1 induced more DNA bending. A smaller average end-to-end distance is particularly evident at lower H1 concentrations. By coating the DNA, H1 molecules effectively screen the repulsive interactions between nucleotides with their positive charges (Figs. 6 D and S13 B) (86). Furthermore, at lower H1 concentrations, HP1 α remain bound to the DNA to stabilize highly bent conformations through phase separation (Fig. 6 B, far left). Therefore, $HP1\alpha$ and H1 can work collaboratively to control and condense DNA.

DISCUSSION

We utilized two recently developed near-atomistic force fields (43,45) to study the stability and structural organization of protein-DNA condensates. The simulations succeeded at resolving the difference in phase behaviors of three chromatin regulators and qualitatively reproducing experimental observations. We discovered that the stability of various condensates could be quantitatively captured with a surprisingly simple, linear model that accounts for protein-protein binding free energy and system net charge. In addition, a ternary system that includes $HP1\alpha$, H1, and DNA with implicit solvation phase separates at room temperature into condensates with a layered organization. This layered organization arises due to the bridging of two phases enriched with H1 and HP1, respectively, by DNA molecules. Finally, we observed that protein condensates could affect DNA conformation, with H1 molecules softening the DNA and HP1 α stabilizing compact structures.

Our results have significant implications on heterochromatin organization in vivo. The layered droplets formed by HP1 α , H1, and DNA could persist with the presence of chromatin. In particular, the higher DNA affinity of H1 molecules could allow them to localize to the interior of the chromatin fiber, where H1 binds near nucleosome dyads and with linker DNA (70). Meanwhile, HP1 α would favor configurations closer to the exterior of the fiber, where it could still recognize H3K9me3 marks (87). Such a layered distribution could facilitate the two molecules to collaboratively soften and compact chromatin. While our focus in this study is on protein-DNA droplets, we hope to extend these models to chromatin structures in the future.

HP1 β destabilizes HP1 α -DNA droplets through heterodimerization

We note that the phase diagram of the ternary system, $1HP1\alpha:1HP1\beta:2DNA$, is not entirely consistent with Please cite this article in press as: Latham and Zhang, On the stability and layered organization of protein-DNA condensates, Biophysical Journal (2022), https:// doi.org/10.1016/j.bpj.2022.03.028

Latham and Zhang

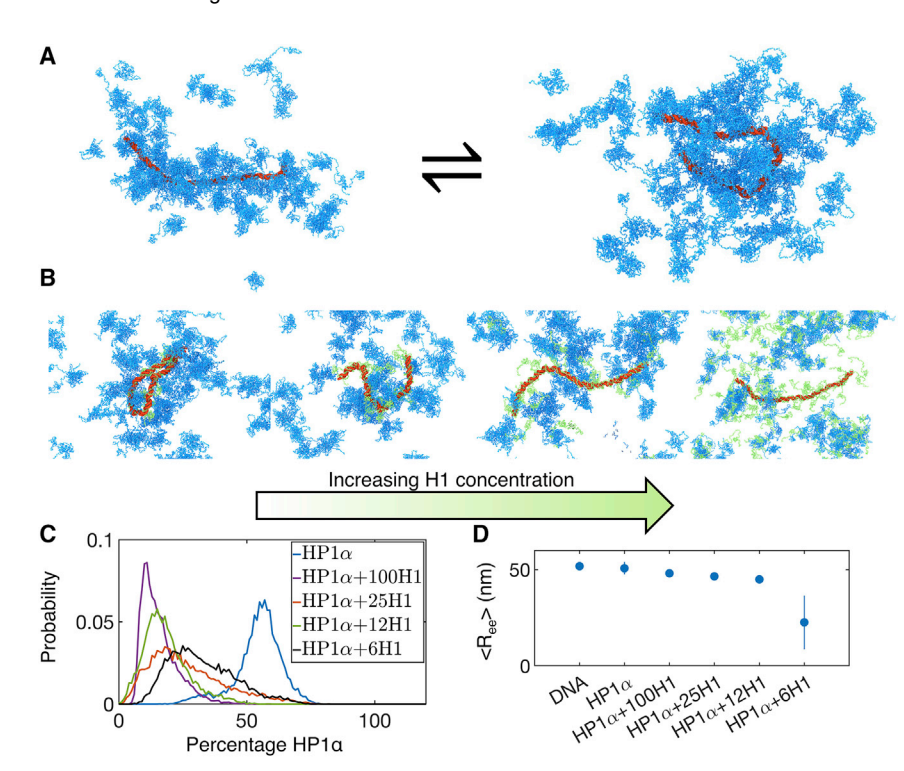


FIGURE 6 Impact of protein droplets on single-DNA conformation. (A) Formation of HP1 (blue) condensates facilitates the transition between extended and compact conformations of a 200-bp-long DNA (red). (B) Snapshots from simulations of $HP1\alpha + H1 + DNA$ mixtures, with the H1 (green) concentration increasing from left to right. (C) Impact of H1 concentration on HP1 α 's participation in cluster formation. Different curves represent probability distributions of the percentage of HP1 α in the system that is incorporated into the largest cluster formed by protein and DNA molecules. (D) Impact of LLPS on the average DNA end-to-end distance ($\langle R_{ee} \rangle$). A simulated result under identical conditions but without proteins is also included for comparison (DNA). Error bars represent standard deviations of the mean. To see this figure in color, go online.

observations made by Keenen et al. (46). The authors found that HP1 β can dissolve HP1 α -DNA droplets, suggesting less stable condensates and a lower $T_{\rm C}$ for the ternary system compared with $HP1\alpha$ -DNA. However, the phase diagrams showed that the two systems share comparable values for $T_{\rm C}$. The discrepancy could arise from the inability of our simulations to capture heterodimerization that might occur on a much slower timescale after the homodimers dissociate. As suggested by Keenen et al. (46), heterodimerization could break the interactions that stabilize HP1 α droplets. To test this hypothesis while avoiding simulating the slow kinetics of heterodimer formation from homodimers, we performed additional simulations in which the HP1 homologs were restricted in heterodimeric conformations. We found that the radius of gyration of the heterodimer lies in between that of HP1 α and HP1 β (Fig. S16) (43).

We computed the phase diagram and $T_{\rm C}$ for pure heterodimers, which we denote as HP1 α /HP1 β , and their DNA mixture (Fig. S17). While the condensate formed by heterodimers is equally stable compared with that of HP1 α and HP1 β homodimers, the stability of the DNA mixture is significantly reduced. However, we still predicted LLPS at room temperature for 1HP1 α /HP1 β :1DNA. While this could be due to the limited resolution of our coarsegrained model, a more likely possibility is the use of a high DNA concentration in our slab simulations. We next turned to simulations with a long, single DNA (Fig. S18), where the protein-DNA ratio is more comparable with the experimental value (46). In these simulations, the heterodimer significantly reduced the percentage of $HP1\alpha$ in the largest cluster formed by protein and DNA molecules relative to homodimer simulations (HP1 α + $HP1\beta$). Therefore, our simulations indeed support heterodimerization as a mechanism to destabilize HP1 α droplets formed with DNA.

SUPPORTING MATERIAL

Supporting material can be found online at https://doi.org/10.1016/j.bpj. 2022.03.028.

AUTHOR CONTRIBUTIONS

A.L. and B.Z. conceived the research, performed the research, analyzed the data, and wrote the paper.

ACKNOWLEDGMENTS

This work was supported by the National Institutes of Health (grant R35GM133580) and the National Science Foundation (grant MCB-2042362). A.L. further acknowledges support by the National Science Foundation Graduate Research Fellowship Program. We thank Dr. Xingcheng Lin for his help in implementing the MRG-CG DNA model.

SUPPORTING CITATIONS

References (88–106) appear in the supporting material.

REFERENCES

- 1. Sabari, B. R., A. Dall'Agnese, and R. A. Young. 2020. Biomolecular condensates in the nucleus. Trends Biochem. Sci. 45:961-977. https:// doi.org/10.1016/j.tibs.2020.06.007.
- 2. Sanulli, S., and G. J. Narlikar. 2020. Liquid-like interactions in heterochromatin: implications for mechanism and regulation. Curr. Opin. Cell Biol. 64:90–96. https://doi.org/10.1016/j.ceb.2020.03.004.
- 3. Banani, S. F., H. O. Lee, ..., M. K. Rosen. 2017. Biomolecular condensates: organizers of cellular biochemistry. Nat. Rev. Mol. Cell Biol. 18:285-298.
- 4. Uversky, V. N. 2017. Intrinsically disordered proteins in overcrowded milieu: membrane-less organelles, phase separation, and intrinsic disorder. Curr. Opin. Struct. Biol. 44:18-30. https://doi.org/10.1016/j. sbi.2016.10.015.
- 5. Hnisz, D., K. Shrinivas, ..., P. A. Sharp. 2017. A phase separation model predicts key features of transcriptional control. Cell. 169:13-23.
- 6. Riback, J. A., C. D. Katanski, ..., D. A. Drummond. 2017. Stress-triggered phase separation is an adaptive, evolutionarily tuned response. Cell. 168:1028-1040.e19. https://doi.org/10.1016/j.cell.2017.02.027.
- 7. Brangwynne, C. P., C. R. Eckmann, ..., A. A. Hyman. 2009. Germline P granules are liquid droplets that localize by controlled dissolution/ condensation. Science. 324:1729-1732.
- 8. Franzmann, T., S. Stoynov, ..., M. Jahnel. 2015. A liquid-to-solid phase transition of the ALS protein FUS accelerated by disease mutation. Cell. 162:1066-1077. https://doi.org/10.1016/j.cell.2015.07.047.
- 9. Lin, X., Y. Qi, ..., B. Zhang. 2021. Multiscale modeling of genome organization with maximum entropy optimization. J. Chem. Phys. 155:010901. https://doi.org/10.1063/5.0044150.
- 10. Larson, A. G., D. Elnatan, ..., G. J. Narlikar. 2017. Liquid droplet formation by HP1α suggests a role for phase separation in heterochromatin. Nature. 547:236-240.
- 11. Strom, A. R., A. V. Emelyanov, ..., G. H. Karpen. 2017. Phase separation drives heterochromatin domain formation. Nature. 547:241-
- 12. Wang, L., Y. Gao, ..., P. Li. 2019. Histone modifications regulate chromatin compartmentalization by contributing to a phase separation mechanism. Mol. Cell. 76:646-659.e6.
- 13. Sabari, B. R., A. Dall'Agnese, ..., Y. E. Guo. 2018. Coactivator condensation at super-enhancers links phase separation and gene control. Science. 361:eaar3958.
- 14. Hennig, S., G. Kong, ..., A. H. Fox. 2015. Prion-like domains in RNA binding proteins are essential for building subnuclear paraspeckles. J. Cell Biol. 210:529-539.
- 15. Kamat, K., Y. Qi, ..., B. Zhang. 2021. Genome compartmentalization with nuclear landmarks: random yet precise. Preprint at bioRxiv. https://doi.org/10.1101/2021.11.12.468401.
- 16. Feric, M., N. Vaidya, ..., C. P. Brangwynne. 2016. Coexisting liquid phases underlie nucleolar subcompartments. Cell. 165:1686-1697. https://doi.org/10.1016/j.cell.2016.04.047.
- 17. Qi, Y., and B. Zhang. 2021. Chromatin network retards droplet coalescence. Nat. Commun. 6824:6824. https://doi.org/10.1101/2021.03.02.
- 18. Ranganathan, S., and E. I. Shakhnovich. 2020. Dynamic metastable long-living droplets formed by sticker-spacer proteins. eLife.
- 19. Espinosa, J. R., J. A. Joseph, ..., R. Collepardo-Guevara. 2020. Liquid network connectivity regulates the stability and composition of biomolecular condensates with many components. Proc. Natl. Acad. Sci. U.S.A. 117:13238-13247.
- 20. Hyman, A. A., C. A. Weber, and F. Jülicher. 2014. Liquid-liquid phase separation in biology. Annu. Rev. Cell Dev. Biol. 30:39-58.
- 21. Boeynaems, S., S. Alberti, ..., M. Fuxreiter. 2018. Protein phase separation: a new phase in cell biology. *Trends Cell Biol.* 28:420–435.

- 22. Rippe, K. 2021. Liquid-liquid phase separation in chromatin. Cold Spring Harb. Perspect. Biol. 14:a040683.
- 23. Choi, J. M., A. S. Holehouse, and R. V. Pappu. 2020. Physical principles underlying the complex biology of intracellular phase transitions. Annu. Rev. Biophys. 49:107-133.
- 24. Dignon, G. L., R. B. Best, and J. Mittal. 2020. Biomolecular phase separation: from molecular driving forces to macroscopic properties. Annu. Rev. Phys. Chem. 71:53-75.
- 25. Turner, A. L., M. Watson, ..., K. Stott. 2018. Highly disordered histone H1-DNA model complexes and their condensates. Proc. Natl. Acad. Sci. U.S.A. 115:11964-11969.
- 26. Joseph, J. A., J. R. Espinosa, ..., R. Collepardo-Guevara. 2021. Thermodynamics and kinetics of phase separation of protein-RNA mixtures by a minimal model. Biophys. J. 120:1219-1230. https://doi. org/10.1101/2020.01.24.916858.
- 27. Sing, C. E., and S. L. Perry. 2020. Recent progress in the science of complex coacervation. Soft Matter. 16:2885-2914.
- 28. Rumyantsev, A. M., N. E. Jackson, and J. J. De Pablo. 2021. Polyelectrolyte complex coacervates: recent developments and new frontiers. Annu. Rev. Condens. Matter Phys. 12:155-176.
- 29. Erdel, F., and K. Rippe. 2018. formation of chromatin subcompartments by phase separation. Biophys. J. 114:2262-2270. https://doi. org/10.1016/j.bpj.2018.03.011.
- 30. Ryu, J. K., C. Bouchoux, ..., C. Dekker. 2021. Bridging-induced phase separation induced by cohesin SMC protein complexes. Sci. Adv. 7:eabe590.
- 31. Brackley, C. A., B. Liebchen, ..., D. Marenduzzo. 2017. Ephemeral protein binding to DNA shapes stable nuclear bodies and chromatin domains. Biophys. J. 112:1085-1093. https://doi.org/10.1016/j.bpj. 2017.01.025.
- 32. Banerjee, P. R., A. N. Milin, ..., A. A. Deniz. 2017. Reentrant phase transition drives dynamic substructure formation in ribonucleoprotein droplets. Angew. Chem. 129:11512-11517.
- 33. Henninger, J. E., O. Oksuz, ..., R. A. Young. 2021. RNA-mediated feedback control of transcriptional condensates. Cell. 184:207-225.e24.
- 34. Regy, R. M., G. L. Dignon, ..., J. Mittal. 2020. Sequence dependent phase separation of protein-polynucleotide mixtures elucidated using molecular simulations. Nucleic Acids Res. 48:12593-12603.
- 35. Fei, J., M. Jadaliha, ..., T. Ha. 2017. Quantitative analysis of multilayer organization of proteins and RNA in nuclear speckles at super resolution. J. Cell Sci. 130:4180-4192.
- 36. Jacobs, W. M., and D. Frenkel. 2017. Phase transitions in biological systems with many components. Biophys. J. 112:683-691.
- 37. Nguemaha, V., and H. X. Zhou. 2018. Liquid-liquid phase separation of patchy particles illuminates diverse effects of regulatory components on protein droplet formation. Sci. Rep. 8:6728. https://doi.org/ 10.1038/s41598-018-25132-1.
- 38. Pal, T., J. Wessén, ..., H. S. Chan. 2021. Subcompartmentalization of polyampholyte species in organelle-like condensates is promoted by charge-pattern mismatch and strong excluded-volume interaction. Phys. Rev. E. 103:042406.
- 39. Harmon, T. S., A. S. Holehouse, and R. V. Pappu. 2018. Differential solvation of intrinsically disordered linkers drives the formation of spatially organized droplets in ternary systems of linear multivalent proteins. New J. Phys. 20:045002.
- 40. Boeynaems, S., A. S. Holehouse, ..., A. D. Gitler. 2019. Spontaneous driving forces give rise to protein-RNA condensates with coexisting phases and complex material properties. Proc. Natl. Acad. Sci. U.S.A. 116:7889–7898.
- 41. Mao, S., D. Kuldinow, ..., A. Košmrlj. 2019. Phase behavior and morphology of multicomponent liquid mixtures. Soft Matter. 15:1297–1311.
- 42. Fyodorov, D. V., B. R. Zhou, ..., Y. Bai. 2018. Emerging roles of linker histones in regulating chromatin structure and function.

Latham and Zhang

- Nat. Rev. Mol. Cell Biol. 19:192–206. https://doi.org/10.1038/nrm. 2017 94
- Latham, A. P., and B. Zhang. 2021. Consistent force field captures homolog resolved HP1 phase separation. *J. Chem. Theor. Comput.* 17:3134–3144.
- Latham, A. P., and B. Zhang. 2022. Unifying coarse-grained force fields for folded and disordered proteins. *Curr. Opin. Struct. Biol.* 72:63–70. https://doi.org/10.1016/j.sbi.2021.08.006.
- Savelyev, A., and G. A. Papoian. 2010. Chemically accurate coarse graining of double-stranded DNA. *Proc. Natl. Acad. Sci. U.S.A.* 107:20340–20345.
- Keenen, M. M., D. Brown, ..., S. Redding. 2021. HP1 proteins compact DNA into mechanically and positionally stable phase separated domains. *eLife*. 10:e64563.
- Benayad, Z., S. Von Bülow, ..., G. Hummer. 2021. Simulation of FUS protein condensates with an adapted coarse-grained model. *J. Chem. Theor. Comput.* 17:525–537.
- Dignon, G. L., W. Zheng, ..., J. Mittal. 2018. Sequence determinants of protein phase behavior from a coarse-grained model. *PLoS Com*put. Biol. 14:e1005941.
- Regy, R. M., J. Thompson, ..., J. Mittal. 2021. Improved coarsegrained model for studying sequence dependent phase separation of disordered proteins. *Protein Sci.* 30:1371–1379.
- Dannenhoffer-Lafage, T., and R. B. Best. 2021. A data-driven hydrophobicity scale for predicting liquid-liquid phase separation of proteins. J. Phys. Chem. B. 125:4046–4056.
- Latham, A. P., and B. Zhang. 2020. Maximum entropy optimized force field for intrinsically disordered proteins. *J. Chem. Theor.* Comput. 16:773–781.
- Tesei, G., T. K. Schulze, ..., K. Lindorff-larsen. 2021. Accurate model of liquid – liquid phase behavior of intrinsically disordered proteins from optimization of single-chain properties. *Proc. Natl. Acad. Sci.* U.S.A. 118:e2111696118.
- Latham, A. P., and B. Zhang. 2019. Improving coarse-grained protein force fields with small-angle X-ray scattering data. *J. Phys. Chem. B*. 123:1026–1034.
- Ding, X., X. Lin, and B. Zhang. 2021. Stability and folding pathways of tetra-nucleosome from six-dimensional free energy surface. *Nat. Commun.* 12:1091. https://doi.org/10.1038/s41467-021-21377-z.
- Kaur, T., M. Raju, ..., P. R. Banerjee. 2021. Sequence-encoded and composition-dependent protein-RNA interactions control multiphasic condensate morphologies. *Nat. Commun.* 12:872. https://doi.org/10. 1038/s41467-021-21089-4.
- Lin, X., R. Leicher, ..., B. Zhang. 2021. Cooperative DNA looping by PRC2 complexes. *Nucleic Acids Res.* 49:6238–6248.
- Parsons, T., and B. Zhang. 2019. Critical role of histone tail entropy in nucleosome unwinding. *J. Chem. Phys.* 150:185103. https://doi.org/ 10.1063/1.5085663.
- Leicher, R., E. J. Ge, ..., S. Liu. 2020. Single-molecule and in silico dissection of the interaction between Polycomb repressive complex 2 and chromatin. *Proc. Natl. Acad. Sci. U.S.A.* 117:30465–30475.
- Farr, S. E., E. J. Woods, ..., R. Collepardo-Guevara. 2021. Nucleosome plasticity is a critical element of chromatin Liquid–Liquid Phase Separation and multivalent nucleosome interactions. *Nat. Commun.* 12:2883. https://doi.org/10.1038/s41467-021-23090-3.
- Tan, C., W. Li, ..., S. Takada. 2015. Modeling structural dynamics of biomolecular complexes by coarse-grained molecular simulations. *Acc. Chem. Res.* 48:3026–3035.
- Moller, J., and J. J. de Pablo. 2020. Bottom-up meets top-down: the crossroads of multiscale chromatin modeling. *Biophys. J.* 118:2057–2065. https://doi.org/10.1016/j.bpj.2020.03.014.
- Watanabe, S., Y. Mishima, ..., S. Takada. 2018. Interactions of HP1 bound to H3K9me3 dinucleosome by molecular simulations and biochemical assays. *Biophys. J.* 114:2336–2351. https://doi.org/10.1016/j.bpj.2018.03.025.

- Källberg, M., H. Wang, ..., J. Xu. 2012. Template-based protein structure modeling using the RaptorX web server. *Nat. Protoc.* 7:1511–1522
- 64. Clementi, C., H. Nymeyer, and J. N. Onuchic. 2000. Topological and energetic factors: what determines the structural details of the transition state ensemble and 'en-route' intermediates for protein folding? An investigation for small globular proteins. *J. Mol. Biol.* 298:937–953.
- Dignon, G. L., W. Zheng, ..., J. Mittal. 2018. Relation between single-molecule properties and phase behavior of intrinsically disordered proteins. *Proc. Natl. Acad. Sci. U.S.A.* 115:9929–9934.
- Berendsen, H. J., D. van der Spoel, and R. van Drunen. 1995. GRO-MACS: a message-passing parallel molecular dynamics implementation. *Comput. Phys. Commun.* 91:43–56.
- Thiru, A., D. Nietlispach, ..., E. D. Laue. 2004. Structural basis of HP1/PXVXL motif peptide interactions and HP1 localisation to heterochromatin. *EMBO J.* 23:489–499.
- Kumar, A., and H. Kono. 2020. Heterochromatin protein 1 (HP1): interactions with itself and chromatin components. *Biophys. Rev.* 12:387–400.
- Bowman, G. D., and M. G. Poirier. 2015. Post-translational modifications of histones that influence nucleosome dynamics. *Chem. Rev.* 115:2274–2295.
- Wu, H., Y. Dalal, and G. A. Papoian. 2021. Binding dynamics of disordered linker histone H1 with a nucleosomal particle. *J. Mol. Biol.* 433:166881.
- Leicher, R., A. Osunsade, ..., S. Liu. 2021. Single-stranded nucleic acid sensing and coacervation by linker histone H1. Preprint at bio-Rxiv. https://doi.org/10.1101/2021.03.17.435841.
- Gibson, B. A., L. K. Doolittle, ..., M. K. Rosen. 2019. Organization of chromatin by intrinsic and regulated phase separation. *Cell*. 179:470–484.
- Munari, F., N. Rezaei-Ghaleh, ..., M. Zweckstetter. 2013. Structural plasticity in human heterochromatin protein 1β. PLoS One. 8:e60887.
- Ackermann, B. E., and G. T. Debelouchina. 2019. Heterochromatin protein HP1α gelation dynamics revealed by solid–state NMR spectroscopy. *Angew. Chem.* 131:6366–6371.
- Shakya, A., S. Park, ..., J. T. King. 2020. Liquid-liquid phase separation of histone proteins in cells: role in chromatin organization. *Biophys. J.* 118:753–764.
- Guo, L., and J. Shorter. 2015. It's raining liquids: RNA tunes viscoelasticity and dynamics of membraneless organelles. *Mol. Cell*. 60:189–192. https://doi.org/10.1016/j.molcel.2015.10.006.
- Zhang, H., S. Elbaum-Garfinkle, ..., A. S. Gladfelter. 2015. RNA controls PolyQ protein phase transitions. *Mol. Cell*. 60:220–230. https://doi.org/10.1016/j.molcel.2015.09.017.
- Elbaum-Garfinkle, S., Y. Kim, ..., C. P. Brangwynne. 2015. The disordered P granule protein LAF-1 drives phase separation into droplets with tunable viscosity and dynamics. *Proc. Natl. Acad. Sci. U.S.A.* 112:7189–7194.
- Overbeek, J. T. G., and M. J. Voorn. 1957. Phase separation in polyelectrolyte solutions: theory OF complex coacervation. *J. Cell Phys*iol. Suppl. 49:7–22.
- Rubinstein, M., and R. Colby. 2003. Polymer Physics. Oxford University Press.
- Zhang, P., K. Shen, ..., Z. G. Wang. 2018. Salt partitioning in complex coacervation of symmetric polyelectrolytes. *Macromolecules*. 51:5586–5593.
- Xu, B., G. He, ..., N. S. Wingreen. 2019. Rigidity enhances a magicnumber effect in polymer phase separation. *Nat. Commun.* 11:1561. https://doi.org/10.1038/s41467-020-15395-6.
- Zumbro, E., and A. Alexander-Katz. 2020. Polymer stiffness regulates multivalent binding and liquid-liquid phase separation. *Biophys. J.* 119:1849–1864. https://doi.org/10.1016/j.bpj.2020.09.035.
- Sanders, D. W., N. Kedersha, ..., C. P. Brangwynne. 2020. Competing protein-RNA interaction networks control multiphase intracellular

- organization. Cell. 181:306-324.e28. https://doi.org/10.1016/j.cell. 2020.03.050
- 85. Atkins, P., J. de Paula, and J. Keeler. 2018. Atkins' Physical Chemistry, 11e edition. Oxford University Press.
- 86. Sridhar, A., S. E. Farr, ..., R. Collepardo-Guevara. 2020. Emergence of chromatin hierarchical loops from protein disorder and nucleosome asymmetry. Proc. Natl. Acad. Sci. U.S.A. 117:7216–7224.
- 87. Nishibuchi, G., S. Machida, ..., J. I. Nakayama. 2014. N-terminal phosphorylation of HP1α increases its nucleosome-binding specificity. Nucleic Acids Res. 42:12498-12511.
- 88. Gowers, R., M. Linke, ..., O. Beckstein. 2016. MDAnalysis: a Python package for the rapid analysis of molecular dynamics simulations. In Proceedings of the 15th Python in Science Conference.
- 89. Bonomi, M., D. Branduardi, ..., M. Parrinello. 2009. PLUMED: a portable plugin for free-energy calculations with molecular dynamics. Comput. Phys. Commun. 180:1961-1972. https://doi.org/10.1016/j. cpc.2009.05.011.
- 90. Wang, S., J. Ma, ..., J. Xu. 2013. Protein structure alignment beyond spatial proximity. Sci. Rep. 3:1448.
- 91. Wang, S., J. Peng, and J. Xu. 2011. Alignment of distantly related protein structures: algorithm, bound and implications to homology modeling. Bioinformatics. 27:2537-2545.
- 92. Kang, J., J. Chaudhary, ..., H. Yua. 2011. Mitotic centromeric targeting of HP1 and its binding to Sgo1 are dispensable for sister-chromatid cohesion in human cells. Mol. Biol. Cell. 22:1181-1190.
- 93. Mehler, E. L., and G. Eichele. 1984. Electrostatic effects in wateraccessible regions of proteins. Biochemistry. 23:3887-3891.
- 94. Mehler, E. L., and T. Solmajer. 1991. Electrostatic effects in proteins: comparison of dielectric and charge models. Protein Eng. Des. Sel. 4:903-910.
- 95. Noel, J. K., M. Levi, ..., P. C. Whitford. 2016. Smog 2: a versatile software package for generating structure-based models. PLoS Comput. Biol. 12:1-14.

- 96. Baumann, C. G., S. B. Smith, ..., C. Bustamante. 1997. Ionic effects on the elasticity of single DNA molecules. Proc. Natl. Acad. Sci. U.S.A. 94:6185–6190.
- 97. Rizzo, V., and J. Schellman. 1981. Flow dichroism of T7 DNA as a function of salt concentration. Biopolymers. 20:2143-2163.
- 98. Michaud-Agrawal, N., E. J. Denning, ..., O. Beckstein. 2011. MDAnalysis: a toolkit for the analysis of molecular dynamics simulations. J. Comput. Chem. 32:2319-2327.
- 99. Privalov, P. L., A. I. Dragan, and C. Crane-Robinson. 2011. Interpreting protein/DNA interactions: distinguishing specific from non-specific and electrostatic from non-electrostatic components. Nucleic Acids Res. 39:2483-2491.
- 100. Shirts, M. R., and J. D. Chodera. 2008. Statistically optimal analysis of samples from multiple equilibrium states. J. Chem. Phys.
- 101. Trzesniak, D., A. P. E. Kunz, and W. F. Van Gunsteren. 2007. A comparison of methods to compute the potential of mean force. ChemPhysChem. 8:162-169.
- 102. Tribello, G. A., F. Giberti, ..., M. Parrinello. 2017. Analyzing and driving cluster formation in atomistic simulations. J. Chem. Theor. Comput. 13:1317-1327.
- 103. Kumar, S., J. M. Rosenberg, ..., P. A. Kollman. 1992. THE weighted histogram analysis method for free-energy calculations on biomolecules. I. The method. J. Comput. Chem. 13:1011-1021.
- 104. Jo, S., T. Kim, ..., W. Im. 2008. CHARMM-GUI: a web-based graphical user interface for CHARMM. J. Comput. Chem. 39:1859-1865.
- 105. Huang, J., S. Rauscher, ..., A. D. MacKerell. 2016. CHARMM36m: an improved force field for folded and intrinsically disordered proteins. Nat. Methods. 14:71-73. https://doi.org/10.1038/nmeth.4067.
- 106. Sawle, L., and K. Ghosh. 2015. A theoretical method to compute sequence dependent configurational properties in charged polymers and proteins. J. Chem. Phys. 143:085101. https://doi.org/10.1063/1. 4929391.